

Measurement and Analysis of High-Frequency Pressure Oscillations in Solid Rocket Motors

P. M. J. Hughes*

Energy, Mines and Resources Canada, Ottawa, Canada
and

E. Cerny†

University of Montreal, Montreal, Canada

During the operation of a solid propellant rocket motor, a high-frequency, finite-amplitude pressure oscillation may develop which is superimposed on the large, time-average chamber pressure. A number of novel techniques to isolate the high-frequency pressure signal from the near-D.C. chamber pressure are described. The hardware to do this consists of off-the-shelf instrumentation modified to give the required characteristics. The software package which is used to display and analyze these high frequency signals is also discussed here. This package will allow the editing and display of the signal in the time and frequency domains and the application of such analytical tools as the fast Fourier transform.

Introduction

AN unstable rocket motor is characterized by a finite-amplitude pressure oscillation superimposed on the larger, near-D.C. chamber pressure. To better understand rocket motor instability and to improve on the prediction of its occurrence, high-resolution pressure data are required from the unstable firing of rocket motors. With these data and the appropriate analytical tools, the rocket motor designer can identify the source of the disturbance in the motor which causes the anomalous behavior and take the steps to eliminate it. Similarly equipped, the theoretician studying the instability can determine empirical constants (such as modal growth rates) or verify his theories.

The high-frequency pressure oscillations are superimposed on the large, near-D.C. chamber pressure and so may be lost in the noise if conventional signal handling techniques are used. A novel technique has been developed¹⁻⁴ to separate the high-frequency wave from the near-D.C. chamber pressure and to analyze the resulting signal. The hardware and software developed for this report were intended for use with piezoelectric type gages; however, with the appropriate modifications, any high-frequency gage system can be used.

The paper is divided into four parts. The first part deals with the problems which may arise when attempting to isolate the small-amplitude wave for analysis. The second part is a comparison of the various techniques undertaken to resolve the problem. The third section describes briefly the computer system developed to analyze the resulting signals. Finally, the last part demonstrates the application of the analytical tools to the pressure signals of some problem motors.

This measurement and analysis technique has been applied to centrally perforated rocket motors with relatively large length-to-diameter ratios. The propellant used was a hydroxyl-terminated polybutadiene binder with ammonium

perchlorate as an oxidizer. The unstable waves studied include both longitudinal nonlinear and transverse acoustic modes. Notwithstanding the above, the measurement and analysis technique described in this paper could be applied to any measurement situation where a low-amplitude, high-frequency signal of interest was superimposed on a large, near-D.C. signal.

The Problem in Separating the High-Frequency Pressure Signal from the Near-D.C. Signal

The acoustic instability itself is sinusoidal in nature and ranges from 50 to 500 kPa in amplitude. This pressure disturbance is superimposed on the time averaged chamber pressure varying from 14 to 35 MPa. Because the frequencies of these waves are tied to the port geometry, the acoustic frequencies range up to about 40 kHz. Furthermore, as the combustion process proceeds, a particular frequency of interest may tend to shift. Therefore, it is necessary to determine not only the actual value of this disturbance frequency, but also its temporal variation, which is of equal importance.

To carry out any kind of study on the signals, it is necessary to digitize them and then perform a fast Fourier transform on the data. The maximum sampling rate obtainable on a standard minicomputer (without direct memory access), including data transfers to disk, is about 15,000 samples per second. However, for 40 kHz signals, using antialiasing filters, and for 80 db alias suppression, the desired sampling

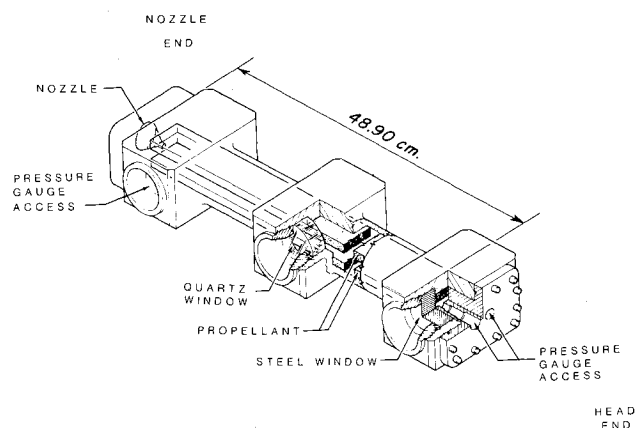


Fig. 1 Schematic of test motor.

Submitted June 7, 1982; presented as Paper 82-1241 at the AIAA/SAE/ASME 18th Joint Propulsion Conference, Cleveland, Ohio, June 21-23, 1982; revision received Aug. 31, 1983. This paper is declared a work of the Canadian Government and therefore is in the public domain.

*Research Scientist, Combustion and Carbonization Research Laboratory, Canadian Centre for Mineral and Energy Technology. Formerly Defense Scientist for the Defense Research Establishment Valcarter.

†Associate Professor, Data Systems and Operations Research.

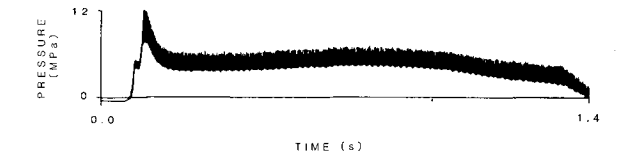


Fig. 2 Chamber pressure as measured at the head end including the near-D.C. component.



Fig. 3 Chamber pressure using the gated technique.

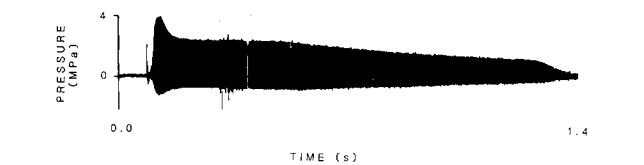


Fig. 4 Chamber pressure using the very short time constant (VSTC) technique.

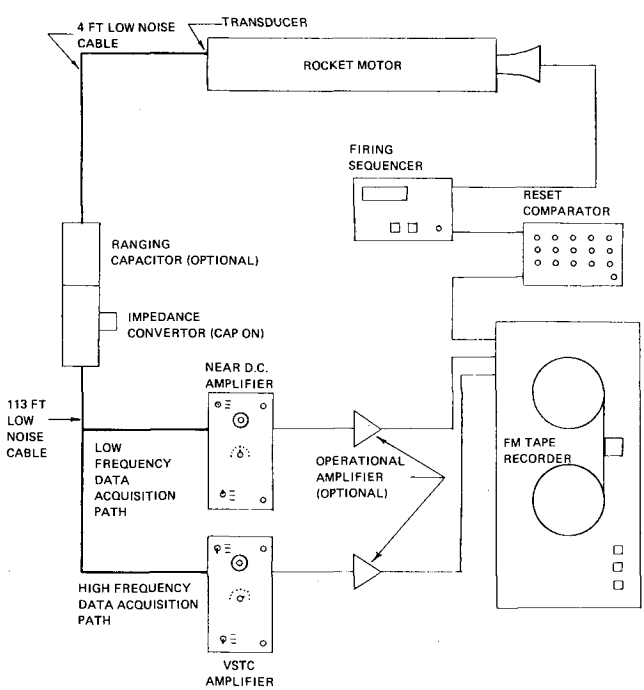


Fig. 5 Optimum setup for high- and low-frequency data acquisition.

rate is 120,000 samples per second. Consequently the signals must be recorded on FM magnetic tape and slowed down 8 to 16 times during playback for digitization.

The near-D.C. portion of the signal must be eliminated from the pressure signal for two reasons. First, since the signal of interest is about 40 db below the near-D.C. signal, the acoustic information would be lost in the noise of the tape recorder, as the signal-to-noise ratio for FM tape recorders is normally about 47 db at 60 ips. Furthermore, the 12 bit A/D converter could provide, at most, seven bits of resolution for

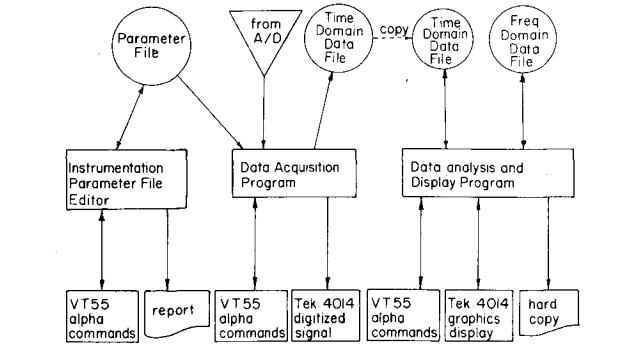


Fig. 6 Application software global organization.

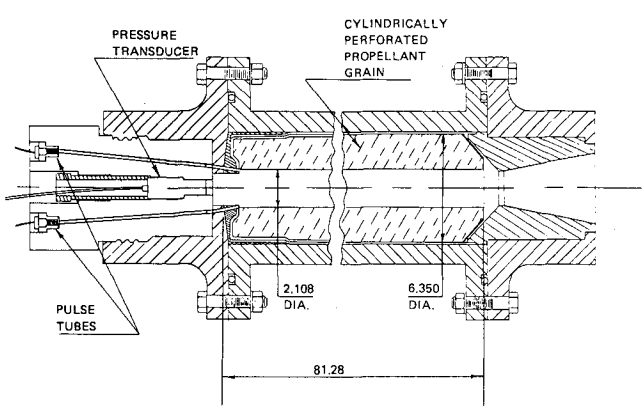


Fig. 7 Demonstration motor layout (dimensions in cm).



Fig. 8 Chamber pressure using the VSTC technique.

the acoustic signal if it were scaled for the high-amplitude, near-D.C. signal. The piezoelectric transducer instrumentation must, therefore, be modified to eliminate the near-D.C. signal. This elimination step must be done without introducing additional noise or distortion since the resulting signal will be further amplified.

Special Hardware for High-Frequency Data Acquisition

Two approaches were attempted to permit isolation and amplification of the signal of interest.^{1,2} One of these, known as the gated technique, consisted of resetting a standard piezotron amplifier [e.g., Sundstand 504E (5)] each time a predetermined threshold value (in the +ve or -ve direction) was attained. This then established a new zero reference for the output signal. The gated method has been reported⁶ as having been used successfully for other applications. The other technique involved a modification² of a standard piezotron amplifier. The feedback resistor ($10^9\Omega$) on the medium time-constant setting of the Sundstand 504E amplifier was changed to $10^6\Omega \pm 5\%$, resulting in a time constant of 2×10^{-4} seconds. This method is called the Very Short Time Constant (VSTC) technique.

To determine the utility of each of the proposed methods, the two measurement techniques were applied to the pressure signals from a rocket motor firing. The rocket motor layout is shown in Fig. 1. The pressure was measured at one of the sidewall port locations. A description of the operating characteristics of the motor is given in the literature⁷⁻¹¹; it is

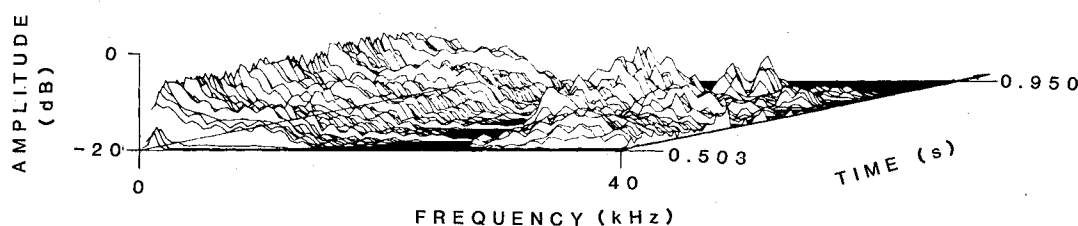


Fig. 9 Three-dimensional display of the power spectrum of the unstable portion of Fig. 8.

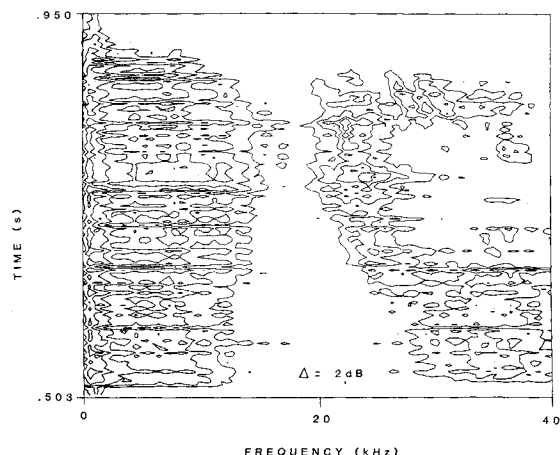
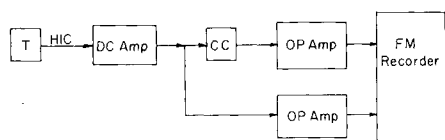


Fig. 10 Contour map of Fig. 9 (the floor at -23 db).



- T -Piezoelectric transducer (eg. Kistler 701-A)
- HIC -High quality cable (high impedance 31 m long)
- DC AMP -Long time constant DC charge amplifier
- CC -Coupling capacitor (typ. 1000 pf)
- OP AMP -Operational amplifier input impedance 1Meg

Fig. 11 Modified setup for high- and low-frequency data acquisition.

sufficient to say that the motor can be fired in such a way as to allow a high-frequency instability to propagate in the combustion chamber. This high-frequency wave is superimposed on the near-D.C. chamber pressure (see Fig. 2).

The signal from the gated circuitry is shown in Fig. 3. The influence of the near-D.C. signal is reduced and the high-frequency signal can be amplified 2.5 times more than without gating. However, the signal is not suitable for direct automated analysis due to its sawtooth carrier. Furthermore, as much as 1 to 2 ms of the signal is lost during the reset period.

The modifications to the amplifier for the VSTC technique gave a low frequency cutoff at either 320 or 800 Hz, depending on the range selected on the amplifier (50 or 20, respectively). Since the resulting amplifier has first-order characteristics, the phase distortion is nearly constant at 180 deg for the frequencies of interest. The VSTC signal measured

during the firing is shown in Fig. 4. The signal amplification improved by a factor of eight for the high-frequency signal as compared to that using an unmodified amplifier. Thus, the VSTC was deemed the preferred approach, and the hardware setup of Fig. 5 was found to be the best configuration to extract a high-frequency, low-amplitude signal for subsequent analysis.

Computer Aided Data Acquisition and Analysis of the Pressure Signal

A variety of computer programs in both Fortran and Machine Language were developed to digitize and then to manipulate the data (such as to apply a fast Fourier transform) in order to analyze the high-frequency information. The software package was developed to run on the DEC PDP-11/34 computer with an AD11-KT A/D converter, KW11-K programmable real-time clock, RK06 disk system (two drives), and an FP-11 floating-point processor as a support for Fortran IV Plus (2). The programs were developed to run in three phases, as indicated in Fig. 6.

The first phase consists of building a parameter file where all the signal channels are described. The description includes transducer sensitivities, cable lengths and capacitances, theoretical calibration constants, and others. The second phase then performs the calibration and signal digitization. The calibration is necessary to determine the static and dynamic characteristics of the system as well as its zero level. The sampling program runs as a privileged task, servicing only the interrupts of the A/D converter programmable clock, ignoring even the system clock. The program takes all the CPU time for itself, locking out all other users, and uses only the disk transfer services of the RSX-11M operating system.² Once the raw data is digitized, it is converted to real pressure or acceleration values by using information from the calibration and from the parameter file.

The third processing phase of the software package consists of an interactive data analysis and display program.³ In this phase, the operator can choose from a long menu of commands to edit or display portions of the signal. It is also possible to perform a fast Fourier transform (FFT) on any part of the signal, with a choice of windowing functions and display modes in the frequency and time domains.

Demonstration of the Technique

The utility of the VSTC technique has been demonstrated in a number of rocket motor firings to date. During the unstable operation of the motor shown in Fig. 7, the VSTC technique was applied to the pressure as measured at the head end. This pressure signal is shown in Fig. 8 as it would be presented using the data analysis and display program. The pressure is shown inverted in this figure. Figure 9 is a three-dimensional display of the FFT of the unstable portion of the pressure signal. Frequency, in kHz is shown along the horizontal axis, amplitude in dB is shown along the vertical axis, and time in seconds along the third axis into the page. The temporal variations of the power spectrum can best be visualized by plotting the three-dimensional data of Fig. 9 in the form of a contour map. This is done in Fig. 10. In this figure, frequency

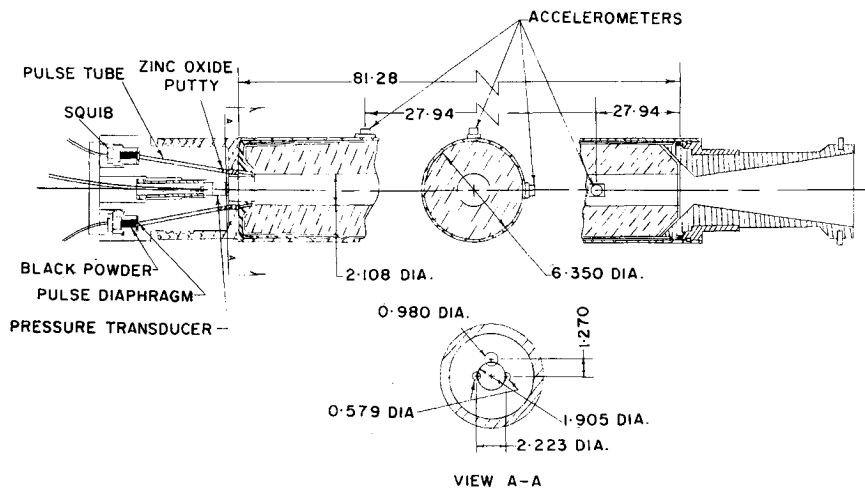


Fig. 12 Rocket motor layout (dimensions in cm).

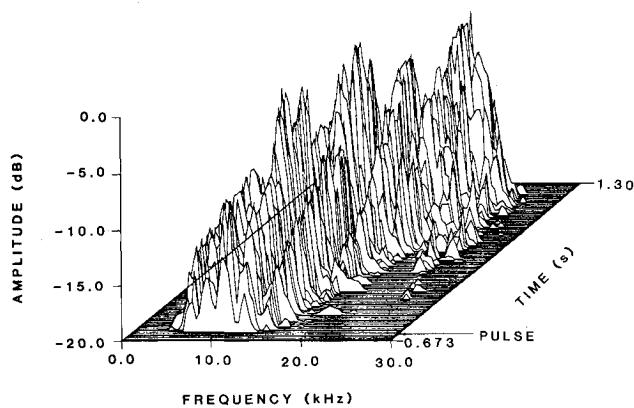


Fig. 13 Power spectrum (FFT) of the signal from the accelerometer near the nozzle during instability.

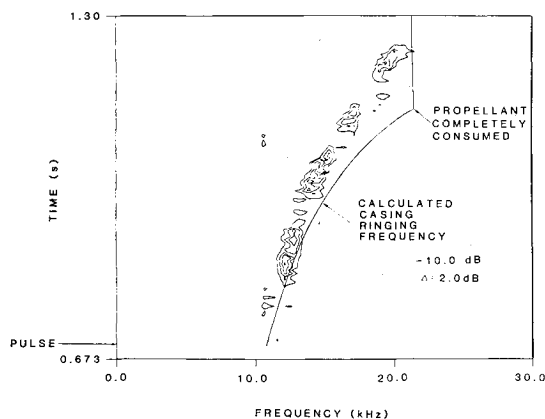


Fig. 14 Contour map of Fig. 13.

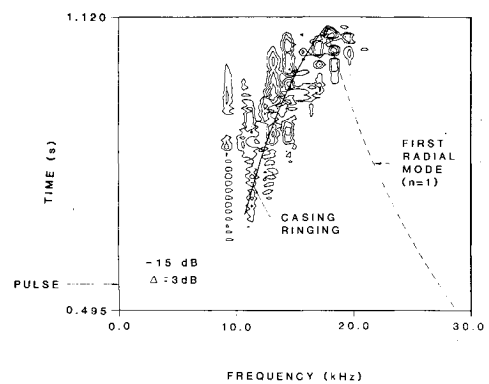


Fig. 15 Contour map of the power spectrum of the accelerometer signal near the head end.

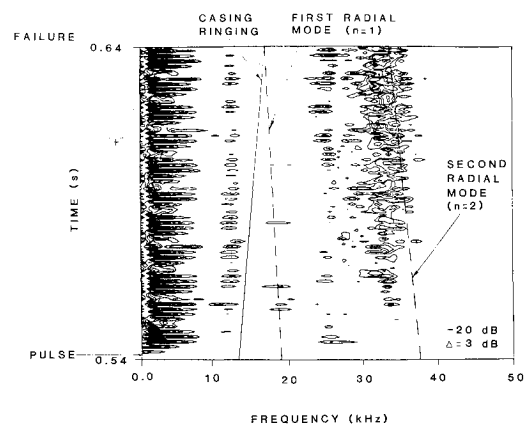


Fig. 16 Contour map of the power spectrum of the pressure signal during unstable operation.

in kHz is shown along the horizontal axis and time in seconds along the vertical axis. The contour lines are lines of constant amplitude in dB. It was with the aid of the display and analysis programming that radial acoustic disturbances were identified in this rocket motor (the contour lines above 20 kHz).

Whereas a suitable hardware setup has been determined to eliminate the near-D.C. signal (Fig. 5), the three-phase data acquisition analysis package can be modified to study signals from firings using other hardware arrangements. A number of rocket motor firings were carried out using the in-

strumentation schematic of Fig. 11. By creating a parametric file containing dummy constants and then simulating the calibration signals with a signal generator, an analysis was performed on the digitized data from these firings. Naturally, the absolute pressure values are not obtainable; however, this poses no problem since the relative amplitude of the spectral peak was of primary interest in these tests.

Figure 12 is the layout of a rocket motor fired with the instrumentation schematic of Fig. 11. A piezoelectric pressure transducer was mounted in the head end and two accelerometers were bonded to the casing at 90 deg to each

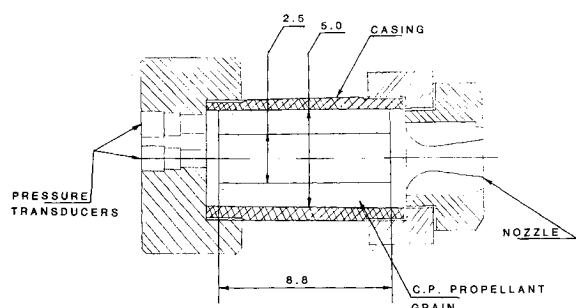


Fig. 17 Burning rate motor (dimensions in cm).

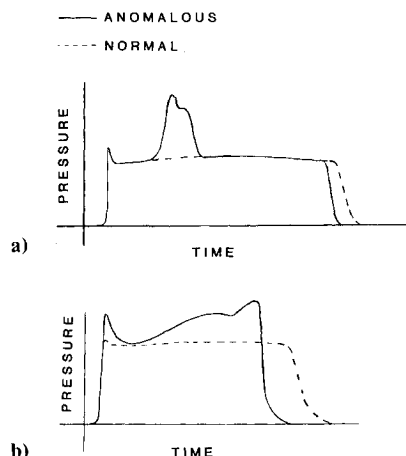


Fig. 18 Anomalous and normal pressure-time curves for burning rate motor.

other. The motor was pulse-driven into the nonlinear type of instability and the resulting pressure and vibration signals were analyzed. Figure 13 shows the frequency domain display of the unstable vibration signal for the accelerometer closest to the nozzle. A shift can be seen towards higher frequencies. Figure 14 is a contour map of Fig. 13, and the trend is more easily seen. The signal measured by the accelerometers has been identified¹² as the free radial vibration (ringing) of the casing in the wake of the shock wave. The trend to higher frequencies is simply the variation of the natural frequency of the casing as the propellant is consumed. The frequency values, their trends, and source were isolated and identified with the aid of the Fourier transform and display programs. An estimation¹² of the variation of the casing ringing frequency is also shown in Fig. 14.

By once again using the Fourier transform analytical package of the software, two failure modes were identified¹² for the motor of Fig. 12. Figure 15 shows the variations of an acoustic mode in the port of the rocket motor and of the casing ringing frequency as measured by an accelerometer. At roughly 1.1 s these frequencies coincided and the motor failed, due to fatiguing of the casing¹² as a result of excitation at its natural frequency. A second failure mode was identified with the aid of the computer techniques. Figure 16 is a contour map of the pressure signal in the frequency domain of a similar rocket motor. At the point marked "+" on the graph the casing dynamics (the solid line) and the port acoustics (the dashed line and the peaks at about 32 kHz) were hypothesized¹² to coincide. The motor became acoustically unstable and the casing burst at 0.64 s.

In the firing of small burning rate motors (Fig. 17), anomalies were noticed in the pressure-time curves (Fig. 18) as measured at the head end. By using the measurement setup of Fig. 11 and subsequent signal analysis, these anomalies were

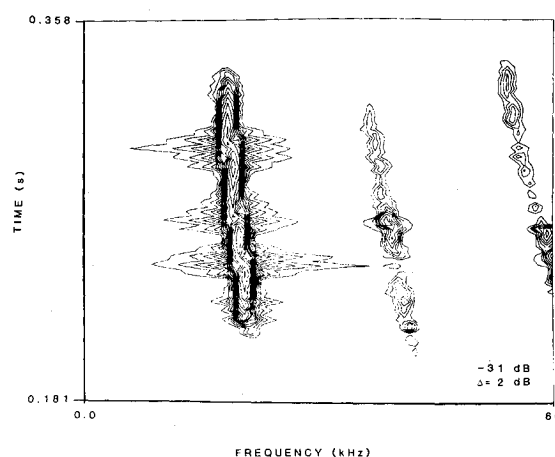


Fig. 19 Contour map of the power spectrum of the unstable portion of the burning rate motor pressure signal ("a" of Fig. 18).

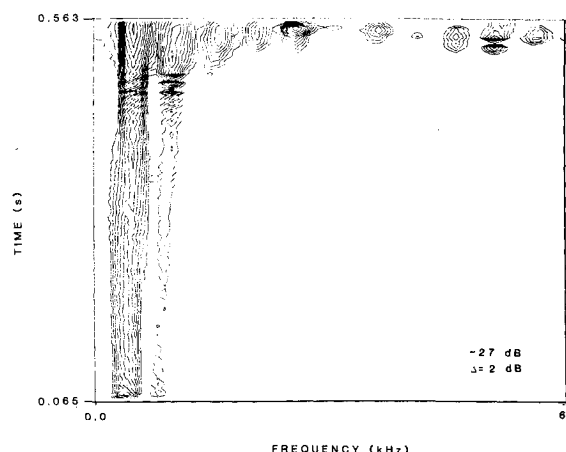


Fig. 20 Contour map of the power spectrum of the unstable portion of the burning rate motor pressure signal ("b" of Fig. 18).

identified as either radial acoustic (Fig. 19) or longitudinal nonlinear (Fig. 20) instabilities.

Conclusion

The development of the hardware and software techniques reported here has greatly enhanced the ability to identify the phenomena involved in the anomalous behavior of rocket motors. Whereas the VSTC hardware technique appears to be the best for the signals of interest, the software is flexible enough to be able to handle data from modified instrumentation. The modifications to be incorporated in the software package in the future include digital filtering subroutines and cross-correlation techniques.

References

- ¹Cerny, E., "Study of Techniques for Data Acquisition and Analysis from Unstable Combustion Experiments," Contract Report No. 1, Defence Research Establishment Valcartier, Department of Supply and Services, Contract No. 3228061, Valcartier, Quebec, Canada, March 1979.
- ²Cerny, E., "Study of Techniques for Data Acquisition and Analysis from Unstable Combustion Experiments," Contract Report No. 2, "Data Acquisition," D.S.S. Contract No. 3228061, Defence Research Establishment Valcartier, Valcartier, Quebec, Canada, July 1979.
- ³Cerny, E., "Study of Techniques for Data Acquisition and Analysis from Unstable Combustion Experiments," Contract Report No. 3, "Data Analysis and Display Software," D.S.S. Contract No. 3228061, Defence Research Establishment, Valcartier, Valcartier, Quebec, Canada, Jan. 1980.

⁴Cerny, E., "Study of Techniques for Data Acquisition and Analysis from Unstable Combustion Experiments," Contract Report No. 4, "Final System Demonstration Experiment," D.S.S. Contract No. 3228061, Defence Research Establishment Valcartier, Valcartier, Quebec, Canada, March 1980.

⁵Instrumentation Manual, "Model 504E Dual Mode Amplifier," Sundstand Data Control Inc., May 1974.

⁶Andrepoint, W., Air Force Rocket Propulsion Laboratory, Private Communication.

⁷Brownlee, W. G. and Kimbell, G. H., "Optical Studies of Longitudinal Combustion Instability," CARDE Technical Note 1708/66, Canadian Armament Research and Development Establishment Valcartier, Valcartier, Canada, May 1966.

⁸Brownlee, W. G. and Kimbell, G. H., "Shock Propagation in Solid Propellant Rocket Combustors," *AIAA Journal*, Vol. 4, June 1966, pp. 1132-1134.

⁹Kimbell, G. H. and Brownlee, W. G., "Flow Processes in Solid Propellant Combustors During Unstable Operation," CARDE Technical Note 1783/68, Canadian Armament Research and Development Establishment Valcartier, Valcartier, Quebec, Canada, March 1968.

¹⁰Brownlee, W. G., "Nonlinear Axial Combustion Instability in Solid Propellant Rocket Motors," *AIAA Journal*, Vol. 2, Feb. 1964, pp. 275-284.

¹¹Kimbell, G. H. and Brownlee, W. G., "Status Report on Optical Studies of Combustion Instability at CARDE," CARDE Technical Note No. 1784/68, Canadian Armament Research and Development Establishment Valcartier, Quebec, Canada, March 1968.

¹²Hughes, P.M.J., "The Influence of the Elasticity of the Casing and Grain on the Combustion Instability of a Solid Rocket Motor," Defence Research Establishment Valcartier (DREV) Memorandum M-2588/81, Sept. 1981.

From the AIAA Progress in Astronautics and Aeronautics Series . . .

SATELLITE COMMUNICATIONS:

FUTURE SYSTEMS-v. 54

ADVANCED TECHNOLOGIES-v. 55

Edited by David Jarett, TRW, Inc.

Volume 54 and its companion Volume 55, provide a comprehensive treatment of the satellite communication systems that are expected to be operational in the 1980's and of the technologies that will make these new systems possible. Cost effectiveness is emphasized in each volume, along with the technical content.

Volume 54 on future systems contains authoritative papers on future communication satellite systems in each of the following four classes: North American Domestic Systems, Intelsat Systems, National and Regional Systems, and Defense Systems. **A significant part of the material has never been published before.** Volume 54 also contains a comprehensive chapter on launch vehicles and facilities, from present-day expendable launch vehicles through the still developing Space Shuttle and the Intermediate Upper Stage, and on to alternative space transportation systems for geostationary payloads. All of these present options and choices for the communications satellite engineer. The last chapter in Volume 54 contains a number of papers dealing with advanced system concepts, again treating topics either not previously published or extensions of previously published works.

Volume 55 on advanced technologies presents a series of new and relevant papers on advanced spacecraft engineering mechanics, representing advances in the state of the art. It includes new and improved spacecraft attitude control subsystems, spacecraft electrical power, propulsion subsystems, spacecraft antennas, spacecraft RF subsystems, and new earth station technologies. Other topics are the relatively unappreciated effects of high-frequency wind gusts on earth station antenna tracking performance, multiple-beam antennas for higher frequency bands, and automatic compensation of cross-polarization coupling in satellite communication systems.

With the exception of the first "visionary" paper in Volume 54, all of these papers were selected from the 1976 AIAA/CASI 6th Communication Satellite Systems Conference held in Montreal, Canada, in April 1976, and were revised and updated to fit the theme of communication satellites for the 1980's. These archive volumes should form a valuable addition to a communication engineer's active library.

Volume 54, 541 pp., 6 × 9, illus., \$19.00 Mem., \$35.00 List

Volume 55, 489 pp., 6 × 9, illus., \$19.00 Mem., \$35.00 List

Two-Volume Set (Vols. 54 and 55), \$38.00 Mem., \$55.00 List

TO ORDER WRITE: Publications Order Dept., AIAA, 1633 Broadway, New York, N.Y. 10019